Published OnlineFirst February 11, 2015; DOI: 10.1158/1078-0432.CCR-14-1998

Clinical Cancer Research

A Translational, Pharmacodynamic, and Pharmacokinetic Phase IB Clinical Study of Everolimus in Resectable Non–Small Cell Lung Cancer

Taofeek K. Owonikoko[1,2], Suresh S. Ramalingam[1,2], Daniel L. Miller[2,3], Seth D. Force[2,3], Gabriel L. Sica[2,4], Jennifer Mendel[2], Zhengjia Chen[2,5], Andre Rogatko[6], Mourad Tighiouart[6], R. Donald Harvey[1,2], Sungjin Kim[2], Nabil F. Saba[1,2], Allan Pickens[3], Madhusmita Behera[1], Robert W. Fu[1], Michael R. Rossi[4,7], William F. Auffermann[8], William E. Torres[8], Rabih Bechara[9], Xingming Deng[2,7], Shi-Yong Sun[1,2], Haian Fu[2,10], Anthony A. Gal[2,4], and Fadlo R. Khuri[1,2]

Abstract

Purpose: The altered PI3K/mTOR pathway is implicated in lung cancer, but mTOR inhibitors have failed to demonstrate efficacy in advanced lung cancer. We studied the pharmacodynamic effects of everolimus in resectable non–small cell lung cancer (NSCLC) to inform further development of these agents in lung cancer.

Experimental Design: We enrolled 33 patients and obtained baseline tumor biopsy and 2[18F]fluoro-2-deoxy-D-glucose-positron emission tomography/computed tomography (FDG-PET/CT) imaging followed by everolimus treatment (5 or 10 mg daily, up to 28 days), or without intervening treatment for controls. Target modulation by everolimus was quantified *in vivo* and *ex vivo* by comparing metabolic activity on paired PET scans and expression of active phosphorylated forms of mTOR, Akt, S6, eIF4e, p70S6K, 4EBP1, and total Bim protein between pretreatment and posttreatment tissue samples.

Results: There were 23 patients on the treatment arm and 10 controls; median age 64 years; 22 tumors (67%) were adenocarcinomas. There was a dose-dependent reduction in metabolic activity (SUV_{max}: 29.0%, −21%, −24%; $P = 0.014$), tumor size (10.1%, 5.8%, −11.6%; $P = 0.047$), and modulation of S6 (−36.1, −13.7, −77.0; $P = 0.071$) and pS6 (−41.25, −61.57, −47.21; $P = 0.063$) in patients treated in the control, 5-mg, and 10-mg cohorts, respectively. Targeted DNA sequencing in all patients along with exome and whole transcriptome RNA-seq in an index patient with hypersensitive tumor was employed to further elucidate the mechanism of everolimus activity.

Conclusion: This "window-of-opportunity" study demonstrated measurable, dose-dependent, biologic, metabolic, and antitumor activity of everolimus in early-stage NSCLC. *Clin Cancer Res; 21(8); 1–10. ©2015 AACR.*

[1]Department of Hematology and Medical Oncology, Emory University, Atlanta, Georgia. [2]Winship Cancer Institute of Emory University, Atlanta, Georgia. [3]Department of Surgery, Emory University, Atlanta, Georgia. [4]Department of Pathology, Emory University, Atlanta, Georgia. [5]Department of Statistics and Bioinformatics, Rollins School of Public Health, Emory University, Atlanta, Georgia. [6]Cedars Sinai Medical Center, Los Angeles, California. [7]Department of Radiation Oncology, Emory University, Atlanta, Georgia. [8]Department of Radiology, Emory University, Atlanta, Georgia. [9]Division of Interventional Pulmonology, Emory University, Atlanta, Georgia. [10]Department of Pharmacology, Emory University, Atlanta, Georgia.

Note: Supplementary data for this article are available at Clinical Cancer Research Online (http://clincancerres.aacrjournals.org/).

T.K. Owonikoko and S.S. Ramalingam contributed equally to this article.

T.K. Owonikoko and S.S. Ramalingam share first authorship of this article.

Corresponding Author: Fadlo R. Khuri, Department of Hematology and Medical Oncology, Emory University and Winship Cancer Institute, Suite C3070, 1365 Clifton Road, NE, Atlanta, GA 30322. Phone: 404-778-4250; Fax: 404-778-5520; E-mail: fkhuri@emory.edu

doi: 10.1158/1078-0432.CCR-14-1998

Introduction

Altered PI3K/AKT/mTOR pathway signaling is implicated in the development and progression of multiple cancers. It has been identified as an early event in lung carcinogenesis in part based on the high expression of activated mTOR pathway protein members in preneoplastic and cancerous lung lesions relative to normal lung tissue.(1–3) However, clinical trials of mTOR pathway targeted inhibitors administered singly or in combination with standard agents such as docetaxel, pemetrexed, gefitinib, and erlotinib in patients with lung cancer have achieved only modest efficacy (4–11). In contrast, demonstrable efficacy of mTOR-targeted agents in breast, kidney, and pancreatic neuroendocrine cancers has led to their regulatory approval in these conditions (12–14). It is currently unknown whether the limited efficacy of mTOR inhibitors in lung cancer compared with other solid tumors reflects a true lack of efficacy, subtherapeutic dosing regimen, or suboptimal clinical trial design in terms of patient selection and endpoints. A better understanding of the biologic activity and optimal administration of mTOR inhibitors in lung

Published OnlineFirst February 11, 2015; DOI: 10.1158/1078-0432.CCR-14-1998

Translational Relevance

This window-of-opportunity phase IB clinical trial studied the pharmacodynamic changes induced by everolimus in previously untreated, resectable non–small cell lung cancer. Using a combination of *in vivo* and *ex vivo* assessments with FDG-PET, immunohistochemistry, and genomic assays, we carefully assessed for evidence of mTOR pathway perturbation in patients treated with an allosteric mTOR inhibitor. Key findings from this work, such as a dose-dependent biologic effect of everolimus and the near complete metabolic and pathologic response in a case of sarcomatoid lung cancer, provide translational insight that will guide future development of this class of agents not only in lung cancer but in other tumor types. In addition, metabolic response and anatomic tumor shrinkage observed in a significant proportion of patients following a short duration of therapy with everolimus suggest potential clinical utility of this agent in well-selected patients with lung cancer.

cancer is therefore necessary if the therapeutic opportunity offered by this class of agents is to be successfully harnessed.

Predictive markers for patient selection and for early determination of long-term therapeutic success are important in the development of targeted biologic agents, including mTOR inhibitors. Robust evidence from preclinical investigations demonstrated a strong correlation between rapalog exposure and modulation of upstream and downstream mediators of the mTOR signaling cascade, leading to the frequent reliance on changes in the activation status of S6, AKT, p70S6, 4E-BP14E-BP1, and eIF4E as readouts of target engagement and efficient signaling abrogation (15, 16). Furthermore, metabolic imaging with positron emission tomography (PET) using ^{18}F-fluorodeoxyglucose (^{18}F-FDG) and ^{18}F-fluoro-thymidine radiotracers has been rigorously evaluated in animal models and human subjects and has shown predictive capability for therapeutic efficacy of mTOR inhibitors (17, 18). These relatively noninvasive tools allow for *in vivo* measurement of biologic activity and are useful as early read-out of the antiproliferative activity that results eventually in long-term efficacy in patients with cancer (17, 18).

The recommended doses for everolimus in early dose-finding studies were 10 mg daily or 70 mg weekly. However, these doses were not defined solely based on toxicity, but on biomarker modulation (S6K) in tumor and surrogate tissues (19, 20). Due to the wide interindividual variability in everolimus exposure (21), it is plausible that a fixed-dose regimen employed in previous lung cancer studies might have been subtherapeutic in up to a third of patients. Because of concerns about additive toxicities, previous studies of everolimus in lung cancer employed a fixed dose of 5 mg, which is lower than the maximum tolerated single-agent dose from phase I testing. To better characterize the activity of mTOR targeting in lung cancer, we conducted this study to assess the safety and pharmacodynamic effects of everolimus in tumor tissue rather than surrogate tissues both *in vivo* and *ex vivo*. Testing the drug in newly diagnosed, previously untreated patients also allowed for evaluation of drug effect in the native tumor devoid of treatment-induced adaptations. This preoperative "window-of-opportunity" trial platform uniquely allows for *in vivo* and *ex vivo* assessment of pathway modulation and antitumor effects.

Materials and Methods

The primary objectives of this phase IB trial were to assess the safety of everolimus in patients with surgically resectable lung cancer and to determine pharmacodynamic (PD) effects of everolimus in patients with previously untreated, surgically resectable, non–small cell lung cancer (NSCLC). The safety endpoint was treatment-emergent toxicity graded according to Common Terminology Criteria for Adverse Events (CTCAE) version 3 criteria and length of hospital stay after surgery. The PD endpoints included metabolic response on paired FDG-PET scan (defined using PERCIST criteria; ref. 22) based on changes in SUV_{max} between baseline and repeat imaging just before surgery), to assess the degree of target modulation as indicated by changes in the activated forms of key protein mediators of mTOR pathway signaling, including Akt, mTOR, p70S6K, 4E-BP1, and p-S6.

Eligibility

Patients were eligible if newly diagnosed with NSCLC of all histologies and deemed to be surgically resectable stage I–IIIA disease. Other eligibility requirements included age $\geq$18 years, ECOG performance status of 0–2, adequate bone marrow function (WBC $\geq$3,000 cells/mm^3, ANC $\geq$1,500 cell/mm^3, platelets $\geq$100,000 cells/mm^3), renal function (creatinine $<1.5 \times$ ULN), hepatic function (bilirubin $\leq 1.5 \times$ ULN, SGOT/SGPT $\leq 2.5 \times$ ULN, alkaline phosphatase $\leq 5 \times$ ULN). Specific exclusion factors included inability to swallow pills, known hypersensitivity to everolimus or any of its excipients; pregnancy or breastfeeding; major intercurrent medical, psychiatric, or social impairment that would limit compliance with study requirements and chronic treatment with systemic steroids or other immunosuppressive agent. The study was conducted under a prospective clinical trial protocol approved by the Emory University IRB (IRB00024810). All enrolled patients were recruited through the multidisciplinary thoracic oncology clinics of Emory Clinic of Emory University (Atlanta, GA). All participants provided a written informed consent before undergoing any protocol-mandated procedures. The study was registered at www.clinicaltrials.gov (NCT00401778); detailed protocol is available on the clinicaltrials.gov reporter website.

Patient selection for treatment administration

Eligible patients were enrolled concurrently on the active and control arms. Patient preference for a specific arm was entertained until the control cohort was completely filled after which all patients were competitively enrolled on the active treatment arm of the study (Fig. 1). For safety reason, enrollment into the active treatment group started with the 5-mg cohort followed by the 10-mg dose cohort in the absence of unanticipated toxicities. Everolimus was self administered by patients at home except on pharmacokinetic samples collection days when the research staff witnessed the drug ingestion before sample collection. Patients on the active treatment arm received everolimus daily continuously for 3 weeks with allowance for an additional week of therapy if necessary to facilitate repeat PET imaging and surgical resection of the tumor, which were mandated to occur within 24 hours of the last dose of everolimus. Patients on the control arm were required to wait for similar amount of time between the baseline and repeat PET scan without receiving any treatment.

Published OnlineFirst February 11, 2015; DOI: 10.1158/1078-0432.CCR-14-1998

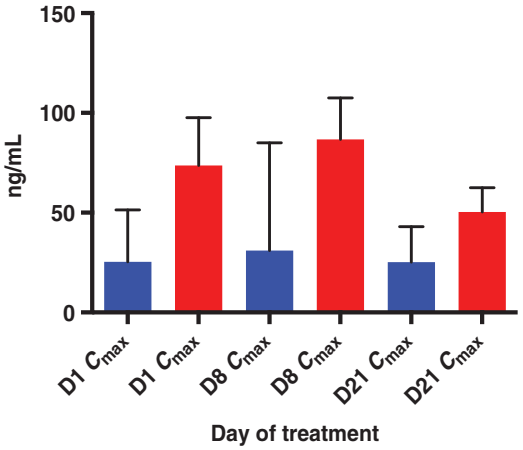

Figure 1.
Everolimus pharmacokinetic characteristics. Bar graphs showing a dose proportional increase in maximum concentration (C_{max}) of everolimus measured in whole blood on days 1, 8, and 21. Blue and red bars represent the 5-mg and 10-mg doses of everolimus, respectively.

Metabolic imaging

All patients had baseline imaging in a fasted state with ^{18}FDG-PET scan and a repeat scan at 3 to 4 weeks later using routine clinical protocol for patient preparation, radiotracer administration, and data acquisition. The repeat imaging occurred no longer than 24 hours before surgical resection.

Pharmacokinetic analysis

Peripheral blood samples for everolimus pharmacokinetic analysis were collected into EDTA tubes on days 1, 8, and 21 at 30 minutes before, and 1, 2, 5, 8, and 24 hours after ingestion of everolimus. Samples were initially stored at 2–8°F during pharmacokinetic collection and subsequently stored within 60 minutes of collection in a −20°F refrigerator, after which all samples were analyzed in a single batch. After high-throughput liquid/liquid extraction, everolimus concentration was measured by a previously validated liquid chromatography/mass spectrometry (LC/MS) method (23). The lower limit of quantification was 0.3 ng/mL. Standard noncompartmental analysis of everolimus was performed using WinNonlin Professional software version 5.2 (Pharsight Corporation) according to the rule of linear trapezoids. Parameters (C_{max}, t_{max}, AUC) were determined and steady state pharmacokinetic measures on days 8 and 21 were compared with those on day 1.

Pharmacodynamic assessment of protein expression in paired tumor tissues

Changes in the expression of key signaling proteins in the mTOR/PI3K pathway were determined by immunohistochemistry using previously published protocols and manufacturers' recommendations for antigen retrieval and antibody dilution along with positive and negative controls. The following primary antibodies were employed at the indicated dilution: S6 (Cell Signaling Technology; cat. No. 2217) at 1:100 dilution, phospho-S6$^{Ser235/236}$ (Cell Signaling Technology; cat. No. 2211) at 1:200 dilution, p70S6 Kinase (Cell Signaling Technology; cat. No. 9202) at 1:100 dilution, phospho-p70S6 Kinase$^{Thr421/Ser424}$ (Cell Signaling Technology; cat. No. 9204) at 1:100 dilution, Akt (Cell Signaling Technology; cat. No. 9272) at 1:200 dilution, phospho-Akt$^{Ser473\ (736E11)}$ (Cell Signaling Technology; cat. No. 3787) at 1:200 dilution, eIF4E (Cell Signaling Technology; cat. No. 9742) at 1:200 dilution, phospho-eIF4E^{Ser209} (Cell Signaling Technology; cat. No. 9741) at 1:200 dilution, 4E-BP1 (Cell Signaling Technology; cat. No. 9452) at 1:200 dilution, phospho-4E-BP1$^{Thr37/46}$ (Cell Signaling Technology; cat. No. 2855) at 1:200 dilution, mTOR (Cell Signaling Technology; cat. No. 2972) at 1:200 dilution, phospho-mTOR$^{Ser2448\ (49F9)}$ (Cell Signaling Technology; cat. No. 2976) at 1:100 dilution, human cytokeratin, clones AE1/AE3 (Dako; cat. No. M3515) at 1:50 dilution and Bim (Cell Signaling Technology; cat. No. 2933) at 1:100 dilution. Two investigators assessed protein expression jointly by light microscopy. The degree of expression was assessed by intensity (0, 1+, 2+, 3+) and percentage of cell staining in line with published algorithm (24). A derivative score (immunoscore) ranging between 0 and 300 was calculated as the product of intensity and percent cell staining.

Targeted DNA sequencing

SNaPshot multiplex sequencing technique was employed to identify known driver mutations in frequently mutated genes in lung cancer, including *AKT1* (c.49G>A), *BRAF* (c.1397G>T, c.1406G>A/C/T, c.1789C>G, c.1799T>A), *EGFR* (c.2156G>A/C, c.2369C>T, c.2573T>G, c.2582T>A, exon.19.del, exon.20.ins), *ERBB2* (ins.A775/exon.20.ins), *KRAS* (c.181C>A/G, c.182A>C/G/T, c.183A>C/T, c.34G>A/C/T, c.35G>A/C/T, c.37G>A/C/T, c.38G>A/C/T, c.180.181TC>CA), *MEK1* (c.167A>C, c.171G>T, c.199G>A), *NRAS* (c.181C>A/G, c.182A>C/G/T), and *PIK3CA* (c.1624G>A/C, c.1633G>A/C,c.3140A>G/T). Sample preparation and genetic mutation identification followed previously described methodologies (25).

Gene expression profiling using RNA-Seq analysis

Tumor samples from a patient with sarcomatoid variant of NSCLC who achieved complete metabolic response and complete pathologic response in the resected tumor specimen were subjected to detailed genetic analysis to identify potential drivers of this response. Total RNA was isolated from FFPE tumor biopsy and resection specimens using the QIAGEN miRNeasy FFPE kit. Total RNA quality and quantity was determined using the Agilent RNA 6000 Nano kits with the Agilent 2100 Bioanalyzer. RNA-Seq library was generated using NuGen Ovation kit by AKESOgen (AKESOgen Inc.). Paired end (100 × 100) sequencing was performed at Beckman Coulter Genomics using an Illumina HISeq2000 instrument. Data quality was assessed on a minimum of 50 million reads per sample using HTQC and FastQC tools. FASTQ reads were aligned to the human reference build 37/hg19 using TopHat alignment. Gene fusions were identified using TopHat Fusion and differential gene expression was performed with CuffDiff.

Statistical analysis

The following statistical assumptions were made with regard to study design and sample size estimate. We wanted to guard against intolerable toxicity in more than 3 patients of 10 treated at each of the 2 doses of everolimus tested in the study. We target the dose such that the probability of intolerable toxicity does not exceed 5%. If four or more patients experienced intolerable toxicity at a given dose, we reject the hypothesis that the

Published OnlineFirst February 11, 2015; DOI: 10.1158/1078-0432.CCR-14-1998

probability of DLT does not exceed 5% for that dose. The probability of observing 4 or more DLTs and incorrectly terminating the trial is 0.00547. The planned accrual is at most 32 eligible patients total, with 10 to 12 patients assigned to receive 5.0 mg/day, 10 patients assigned to 10 mg/day of everolimus, and an additional 10 patients accrued to the control arm. Changes between baseline and repeat measurement for mean SUV_{max} and mean anatomic tumor size were compared by the *t* test and ANOVA. Correlation between metabolic change and tissue-based biomarker modulation was assessed by the Pearson correlation coefficient test. All analyses were performed using SAS statistical package V9.3 (SAS Institute, Inc.). The significance level was set at 0.05 for all tests without correction for multiple comparisons.

Results

Screening, enrollment, and baseline characteristics

We screened 45 patients for enrollment from March 2007 through February 2013. Eight patients withdrew consent before any protocol-mandated procedure and four were screen failures. Based primarily on patient preference and order of enrollment, we assigned 33 consenting and eligible patients with resectable lung cancer to the control (10 patients) or treatment (everolimus—5 mg daily in 12 patients and 10 mg daily in 11 patients) arms. Baseline patient demographics and tumor characteristics are provided in Table 1. Thirty patients (90%) completed all assigned interventions, including paired PET scans (at baseline and within 24 hours of surgery), baseline tissue biopsies, and resected tumor tissue.

Safety

Observation for up to 4 weeks without immediate surgical resection did not result in any major untoward effects in patients on the control arm. A single patient in the control group had premature termination of surgery due to intraoperative finding of mediastinal lymph node involvement, which upstaged the disease stage. The majority of treated patients (17 patients) did not experience any delays in completion of planned interventions and proceeded to surgery within 24 hours of the repeat PET scan. The median and mean time elapsed from end of treatment to surgical resection was 0 and 1 day, respectively (range, 0–7 days). There was a 7-day delay in planned surgical resection in one patient with persistent treatment-related grade 3 diarrhea. Three patients experienced delays of 2 and 3 days in planned surgery due to logistical difficulties with scheduling, while another patient underwent surgery early due to rapid disease progression after only 10 days of everolimus therapy. All other patients proceeded to surgery as planned. Patients in the treatment arm tolerated everolimus. Preoperative adverse events experienced by patients treated with everolimus were mostly anticipated, grade 1 or 2 on the NCI CTCAE grading scale and were managed conservatively. These are summarized by grade and type in Table 2. Notable postsurgical complications considered unrelated to preoperative everolimus therapy included: altered mental status in 2 patients and respiratory failure and prolonged ventilator dependence in the setting of polymicrobial or methicillin-resistant *Staphylococcus aureus* (MRSA) pneumonia leading to tracheostomy in 3 patients. The median and mean length of hospital stay (LOS) after resection was 5 and 8.6 days, respectively (range, 2–43 days). The median LOS was 5 days for both treated (range, 3–43 days) and control patients (range, 2–15 days).

Table 1. Patient demographics, tumor characteristics, and treatment assignment

Variable	Subgroup	*N* (%)
Race	African American	9 (27.27)
	Caucasian	24 (72.73)
Age at enrollment	Mean (±SD)	62 (±9)
	Median (range)	64 (36–77)
Gender	Female	19 (57.58)
	Male	14 (42.42)
Histology	Adenocarcinoma	22 (66.67)
	Others	4 (12.12)
	Squamous	7 (21.21)
Stage	I	14 (42.42)
	II	13 (39.39)
	III	6 (18.18)
Treatment groups	Control	10 (30.3)
	Everolimus (5 mg)	12 (36.36)
	Everolimus (10 mg)	11 (33.33)

NOTE: Total $N = 33$. Data are presented as number of patients (%), mean (±SD), or median (range). Details of patient demographics and characteristics of the tumors according to final pathologic staging and the distribution of patients to control and treatment arms of the study.

Table 2. Treatment-emergent adverse events

Adverse event	Grade 2	Grade 3	Grade 4
Cough	1		
Elevated cholesterol	1		
Elevated creatinine	1		
Weight loss	1		
Elevated alkaline phosphatase	1		
Anemia	3		
Hypophosphatemia	3		
Hypertriglyceridemia	6		
Mouth sores	1		
Sore throat	1		
Rash	3		
Upper respiratory infection	1		
Sinusitis	2		
Hypercalcemia	1		
Urinary frequency	1		
Pain	1	1	
Hypoalbuminemia	1	2	
Hyperglycemia	3	1	
Fatigue	2	1	
Hypokalemia	1	2	
Chest pain	1	1	1
Edema		1	
Hyponatremia		5	
Diarrhea		1	
Respiratory failure			3
MRSA bacteremia			1
Acute renal failure			1

NOTE: Summary of the most frequent adverse events graded according to CTCAE version 3 in patients treated with everolimus.

Everolimus pharmacokinetics

Whole blood samples collected from 12 patients treated with the 5 mg dose and 7 patients treated with the 10 mg dose of everolimus were employed for pharmacokinetics characterization. Day 1 and steady-state concentrations are shown in Table 3. Summary data are reported from steady-state day 8 and 21 values. The median C_{max} at steady state and AUC_{0-24} were dose-proportional, with rapid absorption seen in each group (Fig. 1). There was no significant accumulation at either dose level. Mean half-life in each group was estimated to be 26.5 and 30.3 hours for 5 mg and 10 mg, respectively. The pharmacokinetic characteristics of everolimus determined using extensive sampling on days 1, 8,

Published OnlineFirst February 11, 2015; DOI: 10.1158/1078-0432.CCR-14-1998

Table 3. Everolimus pharmacokinetic analysis parameters

Parameter[a]	5 mg ($n = 12$)	10 mg ($n = 7$)
T_{max} (h)	2 (1–2)	2 (1–2)
Day 1 C_{max} (ng/mL)	29.2 ± 9.9	61.8 ± 26.1
Day 8 C_{min} (ng/mL)	6.3 ± 2.9	17.8 ± 7.6
Day 8 C_{max} (ng/mL)	42.1 ± 17.2	81.8 ± 22.8
Day 21 C_{min} (ng/mL)	5.7 ± 2.3	13.7 ± 9.2
Day 21 C_{max} (ng/mL)	35 ± 15.9	51.5 ± 9.9
Day 8 AUC_{0-24} (ng·h/mL)	210.8 ± 75.9	578.7 ± 186.5
Day 21 AUC_{0-24} (ng·h/mL)	204.7 ± 87.4	506.5 ± 207.6

NOTE: Pharmacokinetic analysis showing dose-proportional increase in C_{min}, C_{max}, and AUC of everolimus when comparing the 5-mg to the 10-mg dose.

and 21 were overall consistent with those previously reported by our group and others (10, 19).

Efficacy

Metabolic response. Comparison of the maximum standardized uptake value (SUV_{max}) from baseline ^{18}F-FDG PET/CT scans and the repeat scan just before surgery was used to assess metabolic response induced by the two different doses of everolimus compared with the untreated patients. Changes in SUV_{max} are expressed as a percent change of initial SUV_{max}. Patients treated with everolimus 5 mg and 10 mg had a mean reduction of 21% and 24%, respectively, in comparison with a mean increase of 29% in control patients ($P = 0.014$); Fig. 2A. Metabolic response classification using PERCIST criteria (22) showed 78% stable metabolic disease (SMD) and 22% progressive metabolic disease (PMD) rates in the control group; 64% SMD and 36% partial metabolic response (PMR) rates in the 5 mg everolimus group; 50% SMD and 50% PMR in the 10 mg everolimus group (Fig. 2B).

Anatomic response. Analysis for objective tumor shrinkage revealed a mean increase in tumor size in the control group and a dose-related reduction in tumor size in everolimus-treated patients; $P < 0.001$; Fig. 2C. In the control arm, 40% of patients met RECIST criteria definition for progression of disease, whereas 60% had stable disease (SD); 18% of patients treated with 5 mg everolimus had best response of progressive disease, whereas 82% achieved SD. Comparatively, 91% of patients in the 10 mg everolimus group had SD and 9% met the RECIST criteria for partial response with 30% tumor shrinkage.

Assessment of target modulation in tissue samples

Expression (immunoscore) of activated phosphorylated S6, p70S6K, eIF4E, AKT, mTOR, and 4E-BP1 was determined by immunohistochemistry in a blinded fashion to provide a readout of target modulation in the enrolled patients. Comparison of expression in baseline and posttreatment surgical samples were significantly different between the treated and control patients with regard to S6 (−36.06 (±100.02), −13.69 (±144.05), −77.03 (±16.02; $P = 0.071$) and pS6 (−41.25 (±65.62), −61.57 (±35.8), −47.21 (±44.96; $P = 0.063$). There was a modest 3% reduction in p-p70S6K expression in control patients, but a 1–2 fold increase in treated patients (Table 4). We, and others, have previously reported the paradoxical activation of p-AKT following inhibition of the mTORC1 complex with rapalogs in preclinical models *in vitro* and *in vivo* (26, 27). The intensity of this paradoxical AKT activation is postulated to correlate with the degree of inhibition of mTORC2 kinase activity, thereby providing a direct measurement of the level of target engagement and pathway modulation. There was a low expression overall of pAKT and insufficient baseline tumor biopsy samples precluded accurate matched comparison. Nonetheless, pAKT immunoscore was overall higher in the posttreatment resected samples, with a stronger magnitude of increase noted for treated patients (Supplementary Fig. S1). Unmatched mean immunoscore for nuclear and cytoplasmic pAKT staining increased more than 40-fold in the treated patients from 0.01 and 0.42, respectively, at baseline to 4.4 and 2.34 posttreatment in the 10 mg cohort; and from 0.3 and 13.1 at baseline to 15 and 47.5 in the 5 mg cohort in comparison with 0.3 and 5.6 at baseline versus 10.9 and 17.5 posttreatment in the control group. There was a significant negative correlation between metabolic response on PET imaging as measured by SUV_{max} and percent change in immunoscore for nuclear p70S6K ($R = -0.685$; $P = 0.029$) and cytoplasmic p70S6K ($R = -0.664$; $P = 0.036$) expression in baseline and posttreatment (Table 5; Supplementary Fig. S2). There was also a negative correlation between anatomic tumor shrinkage and changes in S6 expression ($R = -0.520$; $P = 0.069$) and the ratio of pS6/S6 ($R = -0.633$; $P = 0.067$); Supplementary Fig. S2.

Genetic mutation analysis and correlation with metabolic response

SNaPshot multiplex sequencing was successfully performed in 28 of 33 baseline biopsy samples. Eight of the 28 samples revealed the presence of a genetic mutation, including 6 cases (27%) with *K-Ras* mutation (G12C, G12D, G12V), and 1 case (4%) each of *N-Ras* (Q61L) and *EGFR* (L858R) mutated tumors. The 6 cases with *Ras* gene mutation were fortuitously enrolled either in the control or the everolimus (10 mg) arm of the study. This enabled us to conduct a preliminary hypothesis-generating comparison of metabolic response based on the presence or absence of *RAS* gene mutation. Overall, there was a mean 17% increase in metabolic activity in *Ras*-mutant tumors and a 12% reduction in non–*Ras* mutant tumors ($P = 0.203$). When compared by treatment, *RAS*-mutant tumors in the control group had 88% increase in mean metabolic activity in comparison with a 30% reduction in the *RAS*-mutant tumors treated with everolimus ($P = 0.218$). Conversely, there was a 12% increase versus 21% reduction ($P = 0.039$), respectively, in metabolic activity of non–RAS mutant tumors in the control group and the everolimus (10 mg) group (Fig. 2D).

Sarcomatoid NSCLC response to single-agent everolimus

One patient treated with 10 mg everolimus for 3 weeks attained near complete metabolic response (74% reduction in SUV_{max}) and significant pathologic response with extensive necrosis observed in the resected tumor specimen, consistent with the PET findings (Fig. 3). The patient was a 69-year-old Caucasian woman with approximately 20 pack-year smoking history. She had a biopsy-confirmed sarcomatoid variant of NSCLC and had a 3.6 cm pathologic stage IB (pT2a, N0, M0) sarcomatoid NSCLC postsurgical resection. To elucidate potential genetic alterations responsible for the observed sensitivity of this patient to everolimus, we compared the gene expression profile between the baseline and surgical resection specimen of her tumor with the profile from another patient with similar tumor histology who did not achieve significant metabolic response. We also employed SNaPshot targeted multiplex assay to assess for known driver mutations in *EGFR*, *KRAS*, *NRAS*, *AKT*, *PI3K*, *IDH1*, and *HER2*, as

Published OnlineFirst February 11, 2015; DOI: 10.1158/1078-0432.CCR-14-1998

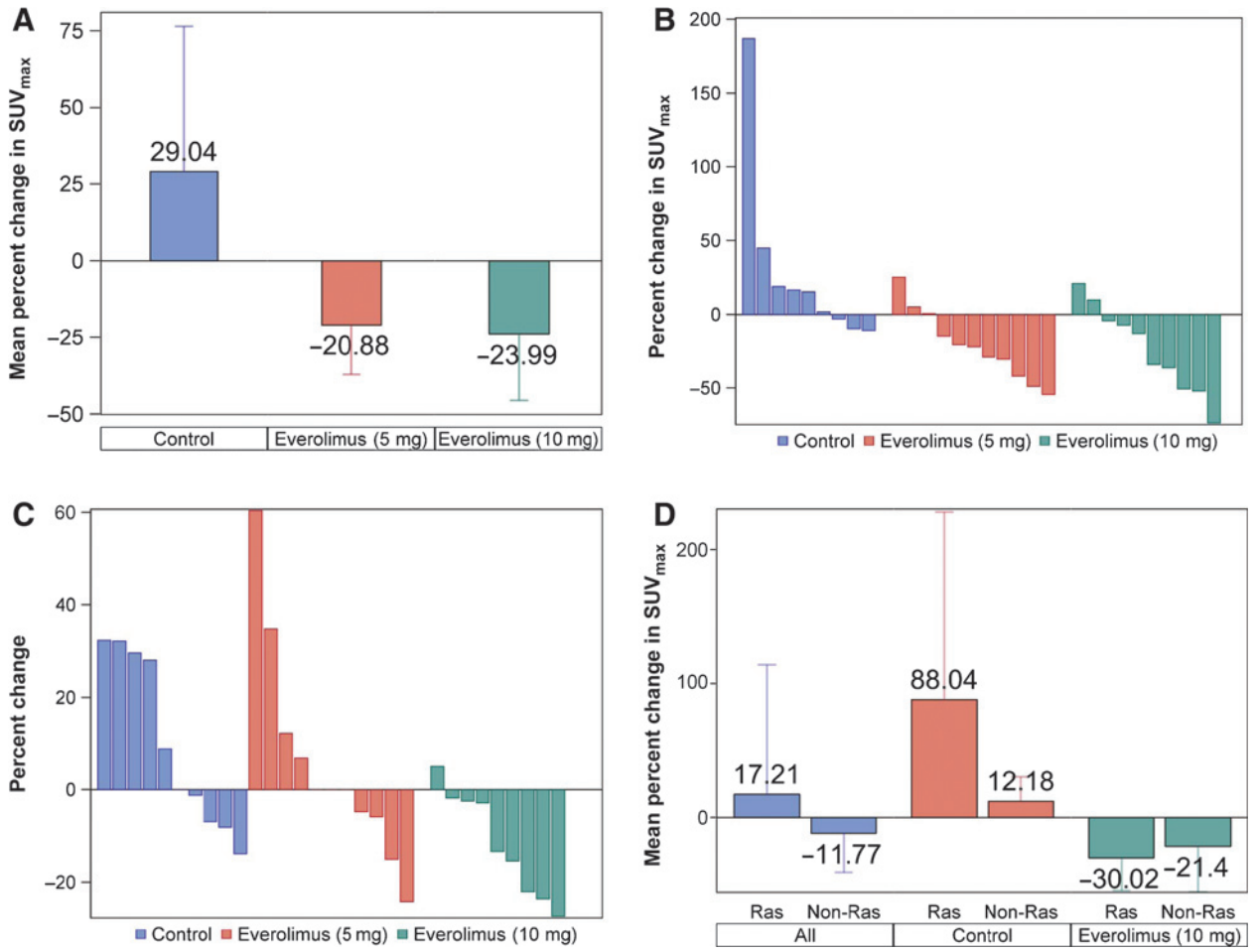

Figure 2.

A, percent change in maximum standardized uptake value (SUV_{max}) on paired PET/CT imaging in different patient groups with reduced metabolic activity in everolimus-treated patients and increased activity in the control group. B, percent change in metabolic activity (measured as SUV_{max}). Waterfall plot of percent change in SUV_{max} on paired PET imaging for individual patients according to treatment group. C, waterfall plot of change in tumor size (measured as maximum tumor diameter) for individual patients by treatment group. D, changes in metabolic activity on paired PET imaging by *RAS* gene mutation status showing comparable activity of everolimus (10 mg) in *RAS*-mutant and nonmutant tumors.

well as RNA-Seq technology to uncover novel mutations and fusion transcripts. The tumor content of the tissue employed for this analysis ranged between 35% and 60% cellularity. The responder had no detectable mutation in the targeted genes included in the SNaPshot panel. However, RNA-Seq deep sequencing and gene expression profile analysis revealed significant differences in the expression pattern of many genes. Supplementary Table S1 lists the top 1% of differentially expressed genes between the responding and the non-responding patients. The full genomic data is available on the dbGAP database under the accession number phs000829.v1.p1 and is directly accessible at this URL: http://www.ncbi.nlm.nih.gov/projects/gap/cgibin/study.cgi?study_id=phs000829.v1.p1.

One gene that was differentially expressed in the posttreatment sample compared with the baseline sample in the responder was the *BCL2L-11* gene that codes for BIM, which showed a 6-fold increase in expression (Fig. 3). There was insufficient pretreatment tissue sample in the majority of cases, including the index case, to conduct immunochemistry to assess baseline BIM expression for this *post-hoc* analysis. However, analysis in available posttreatment samples revealed that BIM expression immunoscore was nearly 2-fold higher in treated patients compared with control patients (84.3 for 5 mg everolimus; 80.5 for 10 mg everolimus vs. 48.6 for control). Moreover, there was a correlation of high BIM expression with a greater reduction in metabolic activity on paired PET scan (Table 5; Pearson correlation coefficient: −0.390; $P = 0.073$ and Supplementary Fig. S2).

Discussion

This phase IB window-of-opportunity study demonstrated robust biologic effects of everolimus in a cohort of patients with early-stage NSCLC. These patients had not received prior systemic anticancer therapy. We were thus able to assess the effect of everolimus on the natural cancer cell phenotype unaltered by compensatory genetic and molecular adaptations induced by systemic anticancer therapy. The common practice of first testing novel investigational agents in heavily pretreated patients might

Published OnlineFirst February 11, 2015; DOI: 10.1158/1078-0432.CCR-14-1998

Table 4. Tissue-based analysis of mTOR pathway protein modulation

Parameter	Overall percent change for all patients	P^a	Dose of everolimus, mg			P^b	P^c
			0	5	10		
S6	−49.21 (±86.59)	**0.045**	−36.06 (±100.02)	−13.69 (± 144.05)	−77.03 (±16.02)	0.510	**0.071**
pS6	−48.59 (±46.7)	**0.002**	−41.25 (±65.62)	−61.57 (± 35.8)	−47.21 (±44.96)	0.866	**0.063**
pS6/S6	62.85 (±208.1)	0.365	−85.75 (±20.15)	−100 (±NA)	128.57 (±219.26)	0.350	0.297
pMTOR	−17.42 (±113.57)	0.622	−6.58 (±138.88)	30 (± 153.95)	−63.82 (±51.3)	0.592	0.608
p4E-BP1	−56.39 (±84.35)	0.101	−95.37 (±4.24)	150 (±NA)	−78.75 (±14.36)	<**0.001**	0.564
p70s6k	55.17 (±312.26)	0.633	25 (±176.78)	137.14 (± 442.07)	−78.62 (±22.79)	0.780	0.757
p70s6k cytoplasmic	161.44 (±513.8)	0.322	−19.17 (±73.16)	0.56 (± 14.93)	305.37 (±686.3)	0.645	0.459
p70s6k nuclear	145.51 (±329.17)	0.173	−3.33 (±100.17)	135 (± 49.5)	223.43 (±437.7)	0.670	0.158
pe1f4e	−22.88 (±49.67)	0.139	−50 (±86.6)	2.78 (± 5.56)	−27.13 (±42.17)	0.406	0.220
PAKT nuclear	−16.67 (±40.82)	0.363	−33.33 (±57.74)	NA	0 (±0)	0.374	0.850
PAKT cytoplasmic	87.5 (±331.39)	0.480	200 (±469.04)	NA	−25 (±50)	0.377	0.505
Bim	−19.26 (±49.3)	0.492	−11.76 (±NA)	NA	−21.76 (±60.07)	0.899	0.766

NOTE: Changes in the expression level of phosphorylated forms of key protein molecules in the mTOR signaling pathway and the proapoptotic protein BIM (measured as percent change in immunoscore between posttreatment samples relative to baseline) between baseline and surgical resection specimens. Data are presented as mean (±SD). Boldface indicates statistical significance.

Abbreviation: NA, not available.

[a]*P* value is calculated by the *t* test for the percent change.

[b]*P* value is calculated by ANOVA for the percent change.

[c]*P* value is calculated by ANOVA for absolute values for pre- and postmeasurements.

confound the ability to demonstrate the expected clinical efficacy. Prior therapies can induce cellular adaptations, some of which might not be critical for the natural development and progression of cancer, but can nonetheless impact the biologic activity of the anticancer agent (28). This limitation is especially germane to the current clinical practice paradigm of precision medicine, where accurate replication of the preclinical model is important for successful clinical translation.

Our study demonstrates the safety, feasibility, and biologic advantages of "window-of-opportunity" studies in patients with early-stage NSCLC. More than 90% of enrolled patients completed the planned interventions and proceeded to successful surgical resection, similar to the experience in the preoperative study of pazopanib in patients with early-stage lung cancer where 86% of enrolled patients completed the intervention and proceeded to surgery (29). Furthermore, our study demonstrates the willingness of newly diagnosed patients with lung cancer to participate in this type of trial, with 33 (74%) of 45 patients screened consenting to participate, despite understandable concerns regarding potential delay in initiating treatment. Our results successfully addressed several key aspects of mTOR inhibitor efficacy in general and specifically in patients with lung cancer. Although everolimus is approved at both the 5 and 10 mg doses for various indications (19, 20), we showed that the 5 mg dose was less potent than the 10 mg dose in modulating key signaling proteins in the PI3K/AKT/mTOR pathway and in inducing metabolic response or anatomic tumor shrinkage. The 10 mg dose of everolimus induced a stronger p-AKT expression concomitant with greater reduction in the downstream read-outs of pathway inhibition in comparison to the 5 mg dose, suggesting that the higher dose is the optimal choice to employ for efficacy studies, at least in patients with NSCLC. It is noteworthy that nearly all the previous trials of everolimus in lung cancer recommended or utilized the 5 mg dose. This potentially suboptimal dose selection could have contributed to the failure of these early-phase studies to demonstrate significant clinical benefit (4, 6, 9, 11, 30). Interestingly, a dose–response trend was observed in a phase IB study of everolimus when combined with paclitaxel in advanced small-cell lung cancer (7), similar to our findings of superior metabolic and anatomic tumor response with the 10 mg dose of everolimus.

Table 5. Correlation of tissue-based pharmacodynamic biomarkers and metabolic changes on PET

Variable	Pearson CC	*P*
S6	0.451	0.106
pS6	0.181	0.555
pS6/S6	−0.038	0.917
pMTOR	−0.140	0.699
p4E-BP1	0.353	0.437
p70s6k	0.154	0.742
p70s6k cytoplasmic	−0.664	**0.036**
p70s6k nuclear	−0.685	**0.029**
pe1f4e	0.396	0.229
PAKT cytoplasmic	0.252	0.585
BIM immunoscore	−0.318	0.682
BIM expression in posttreatment samples	−0.390	**0.073**

NOTE: There was negative correlation between p70S6K (cytoplasmic and nuclear) and changes in metabolic activity on PET imaging. BIM expression in resected posttreatment surgical specimen also showed a modest negative correlation with percent change in SUV_{max} on PET imaging ($P = 0.073$). Boldface indicates statistical significance.

Detailed characterization of patients who achieved unexpected clinical benefit of novel agents is a well-honed research paradigm that has led to the identification of molecular subsets of lung cancer such as EGFR-mutant and ALK- or ROS1 gene rearranged lung cancer (31–33). Similarly, TSC1 mutation was identified as a sensitizing genetic aberration in a patient with bladder cancer with an unexpected complete response to treatment with everolimus (34). Sarcomatoid variant of NSCLC is a particularly aggressive disease with very poor clinical outcomes. The exquisite sensitivity of a patient with sarcomatoid NSCLC to a short duration of treatment with single-agent everolimus prompted the detailed characterization of the molecular and genetic phenotype of the tumor. We observed a 6-fold increased expression of the *BCL2L-11* gene that codes for BIM protein, a proapoptotic member of the Bcl2 protein family. Preclinical models of kinase addicted cancers such as Bcr-abl–addicted leukemia, EGFR-mutant lung cancer, and HER2 kinase-addicted breast cancers demonstrated that activated BIM is required for apoptosis and clinical efficacy of these inhibitors (35–39). Furthermore, baseline BIM protein expression was shown to be a strong predictor of efficacy of kinase inhibitors, including agents targeting the mTOR pathway (35).

Published OnlineFirst February 11, 2015; DOI: 10.1158/1078-0432.CCR-14-1998

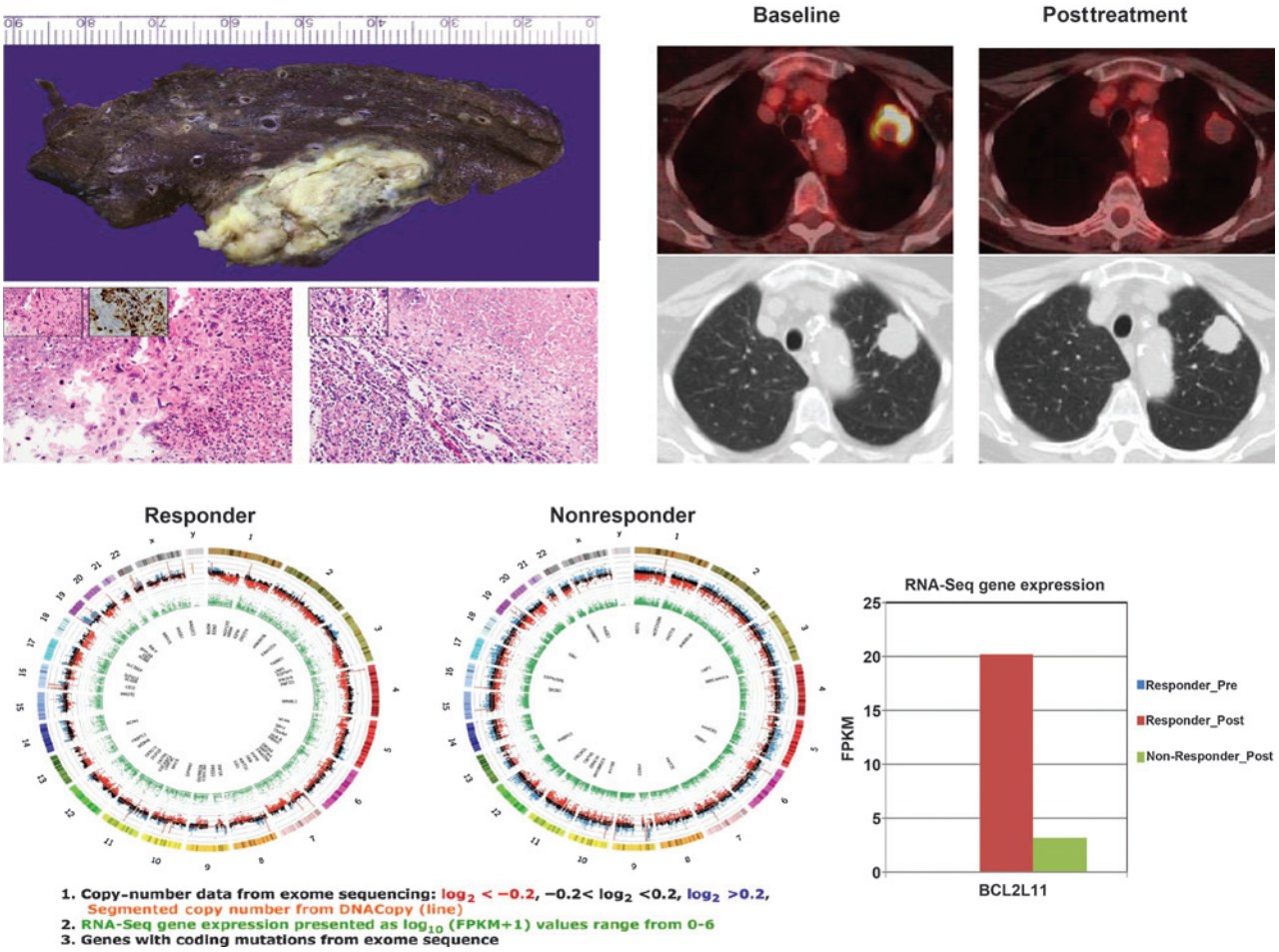

Figure 3.

Major pathologic response and near complete metabolic response in a patient with poorly differentiated, sarcomatoid NSCLC following 4 weeks of everolimus at 10 mg daily dose. Left top, coagulative tumor necrosis in the resected specimen along with histologic sections from baseline biopsy (left, 200×) and posttreatment surgical sections (right, 100×) from a patient with near complete metabolic response to everolimus (10 mg daily for 21 days). Note the extensive tumor necrosis in the posttreatment section. Insets show sarcomatoid cellular morphology (400×) and positive pancytokeratin staining (400×) on immunohistochemistry. Right top: baseline (left) and posttreatment (right) FDG-PET and corresponding CT scan images showing near complete metabolic response in a sarcomatoid NSCLC patient treated with everolimus. Bottom, circos plots of exome and whole transcriptome RNA-seq of the posttreatment sample from the patient with near complete metabolic and pathologic response and another patient with sarcomatoid tumor that did not respond to everolimus (nonresponder). 1, outer circle depicts copy number derived from exome sequencing. The $\log_2$ ratio of total reads per exon divided by median reads across all samples is shown on a *y*-axis ranging from −1 to 1.5. Reads with $\log_2$ ratio of <−0.2 are red, those with $\log_2$ ratio of >0.2 are blue, and those between −0.2 and 0.2 are black. An orange line of the segmented copy number generated using the DNACopy algorithm overlays this data. 2, green inner ring shows RNA-Seq gene expression presented as $\log_{10}$ (FPKM+1) values range from 0–6. 3, the inner circle lists genes with coding mutations identified by exome sequence. Mutations had to be exonic, nonsynonymous, indel, or splice site mutations that had at least 20× coverage with >10% variant reads. This list was parsed to exclude SNPs, SNV, that were not >1% of EVS or 1,000 genomes, not in 100% of reads, and had to have a COSMIC ID. The full genomic data are available on the dbGAP database under the accession number phs000829.v1.p1 and is directly accessible at this URL: http://www.ncbi.nlm.nih.gov/projects/gap/cgibin/study.cgi?study_id=phs000829.v1.p1.

Indeed, a deletion polymorphism in the *BCL2L-11* gene resulting in preferential transcription of the non BH3-containing splice variant of BIM, which is incapable of activating the apoptosis cascade, has also been implicated in *de novo* resistance to kinase inhibitors (40). Mechanistic interrogation of BIM and other Bcl2 family proteins in relation to mTOR inhibitor sensitivity in lung cancer cell lines is currently ongoing in our lab to further explore this finding.

KRAS gene activation resulting from exon 12 coding sequence mutation has been shown to negatively impact the efficacy of PI3K/mTOR pathway–targeted agents in preclinical animal models and was therefore proposed as a potential biomarker in human subjects (41, 42). In a preliminary comparison of metabolic changes in the 6 patients with *RAS*-mutant tumors to those with non–*RAS* mutant tumors in our patient population, we observed similar degree of modulation by FDG-PET imaging. These data are insufficient to conclude that mTOR inhibitor is clinically effective in RAS-mutant tumors. Potential explanations for this observation include the possibility that our patients harbor other genetic alterations not included in our mutation screen panel. One such example is loss of *LKB1* gene, which is present in approximately 30% of patients with adenocarcinoma subtype of NSCLC (3, 43) and whose co-occurrence with *KRAS* mutation was shown to preserve the sensitivity of *KRAS*-mutant cell lines to

Published OnlineFirst February 11, 2015; DOI: 10.1158/1078-0432.CCR-14-1998

mTOR-targeted agents (42). In addition, our approach of evaluating the efficacy of everolimus in previously untreated subjects could have allowed us to observe this activity of everolimus in KRAS-mutant tumors similar to other published reports of mTOR inhibitor activity in previously untreated lung cancer tumors harboring the G12F *KRAS* mutation (11). In conclusion, using the window-of-opportunity platform, tissue-based analysis and metabolic imaging, we established that the 10 mg dose of everolimus modulated the targets more effectively than the lower dose of 5 mg in NSCLC. Future evaluation of this agent in lung cancer should strive to use the maximum dose of 10 mg of everolimus to ensure optimal biologic effect.

Disclosure of Potential Conflicts of Interest

S.S. Ramalingam reports receiving commercial research grants and speakers bureau honoraria from and is a consultant/advisory board member for Novartis. D.L. Miller is a consultant/advisory board member for Ethicon Inc. R.D. Harvey reports receiving commercial research grants from Novartis. No potential conflicts of interest were disclosed by the other authors.

Authors' Contributions

Conception and design: T.K. Owonikoko, S.S. Ramalingam, S.D. Force, Z. Chen, A. Rogatko, M. Tighiouart, R.D. Harvey, S.-Y. Sun, F.R. Khuri

Development of methodology: T.K. Owonikoko, S.S. Ramalingam, M.R. Rossi, H. Fu, F.R. Khuri

Acquisition of data (provided animals, acquired and managed patients, provided facilities, etc.): T.K. Owonikoko, S.S. Ramalingam, S.D. Force, G.L. Sica, J. Mendel, R.D. Harvey, N.F. Saba, A. Pickens, R.W. Fu, M.R. Rossi, W.E. Torres, R. Bechara, X. Deng

Analysis and interpretation of data (e.g., statistical analysis, biostatistics, computational analysis): T.K. Owonikoko, S.S. Ramalingam, S.D. Force, J. Mendel, Z. Chen, M. Tighiouart, R.D. Harvey, S. Kim, M. Behera, M.R. Rossi, W.F. Auffermann, S.-Y. Sun, A.A. Gal

Writing, review, and/or revision of the manuscript: T.K. Owonikoko, S.S. Ramalingam, D.L. Miller, Z. Chen, R.D. Harvey, S. Kim, N.F. Saba, M. Behera, W.F. Auffermann, R. Bechara, X. Deng, H. Fu, F.R. Khuri

Administrative, technical, or material support (i.e., reporting or organizing data, constructing databases): T.K. Owonikoko, S.S. Ramalingam, J. Mendel, R.D. Harvey, N.F. Saba, M. Behera, R.W. Fu

Study supervision: T.K. Owonikoko, S.S. Ramalingam, D.L. Miller, Z. Chen, R.D. Harvey, N.F. Saba, F.R. Khuri

Acknowledgments

The authors thank Jaqueline Rogerio and John Hohneker for their assistance with pharmaceutical support for the study. The authors also thank Anthea Hammond, PhD, for editorial assistance; Charles Butler, BA, for his role in tissue sample collection from patients; and Dianne Alexis, MSC, for her role in performing the immunohistochemical staining. Novartis Oncology generously provided everolimus to all patients.

Grant Support

This work was supported by NIH program project grant P01 CA116676 and 3P01 CA116676-05S1 (to F.R. Khuri), Department of Defense Grant Award W81XWH-05-2-0027 (to F.R. Khuri), and Distinguished Cancer Researcher Award from Georgia Research Alliance (to T.K. Owonikoko, S.S. Ramalingam, G.L. Sica, S.-Y. Sun, and F.R. Khuri).

The costs of publication of this article were defrayed in part by the payment of page charges. This article must therefore be hereby marked *advertisement* in accordance with 18 U.S.C. Section 1734 solely to indicate this fact.

Received November 5, 2014; revised December 23, 2014; accepted January 28, 2015; published OnlineFirst February 11, 2015.

References

1. Tsao AS, McDonnell T, Lam S, Putnam JB, Bekele N, Hong WK, et al. Increased phospho-AKT (Ser(473)) expression in bronchial dysplasia: implications for lung cancer prevention studies. Cancer Epidemiol Biomarkers Prev 2003;12:660–4.
2. Balsara BR, Pei J, Mitsuuchi Y, Page R, Klein-Szanto A, Wang H, et al. Frequent activation of AKT in non-small cell lung carcinomas and preneoplastic bronchial lesions. Carcinogenesis 2004;25:2053–9.
3. Sanchez-Cespedes M, Parrella P, Esteller M, Nomoto S, Trink B, Engles JM, et al. Inactivation of LKB1/STK11 is a common event in adenocarcinomas of the lung. Cancer Res 2002;62:3659–62.
4. Ramalingam SS, Owonikoko TK, Behera M, Subramanian J, Saba NF, Kono SA, et al. Phase II study of docetaxel in combination with everolimus for second- or third-line therapy of advanced non-small-cell lung cancer. J Thorac Oncol 2013;8:369–72.
5. Milton DT, Riely GJ, Azzoli CG, Gomez JE, Heelan RT, Kris MG, et al. Phase 1 trial of everolimus and gefitinib in patients with advanced nonsmall-cell lung cancer. Cancer 2007;110:599–605.
6. Papadimitrakopoulou VA, Soria JC, Jappe A, Jehl V, Klimovsky J, Johnson BE. Everolimus and erlotinib as second- or third-line therapy in patients with advanced non-small-cell lung cancer. J Thorac Oncol 2012;7:1594–601.
7. Sun JM, Kim JR, Do IG, Lee SY, Lee J, Choi YL, et al. A phase-1b study of everolimus plus paclitaxel in patients with small-cell lung cancer. Br J Cancer 2013;109:1482–7.
8. Vansteenkiste J, Solomon B, Boyer M, Wolf J, Miller N, Di Scala L, et al. Everolimus in combination with pemetrexed in patients with advanced non-small cell lung cancer previously treated with chemotherapy: a phase I study using a novel, adaptive Bayesian dose-escalation model. J Thorac Oncol 2011;6:2120–9.
9. Riely GJ, Kris MG, Zhao B, Akhurst T, Milton DT, Moore E, et al. Prospective assessment of discontinuation and reinitiation of erlotinib or gefitinib in patients with acquired resistance to erlotinib or gefitinib followed by the addition of everolimus. Clin Cancer Res 2007;13:5150–5.
10. Ramalingam SS, Harvey RD, Saba N, Owonikoko TK, Kauh J, Shin DM, et al. Phase 1 and pharmacokinetic study of everolimus, a mammalian target of rapamycin inhibitor, in combination with docetaxel for recurrent/refractory nonsmall cell lung cancer. Cancer 2010;116:3903–9.
11. Price KA, Azzoli CG, Krug LM, Pietanza MC, Rizvi NA, Pao W, et al. Phase II trial of gefitinib and everolimus in advanced non-small cell lung cancer. J Thorac Oncol 2010;5:1623–9.
12. Baselga J, Campone M, Piccart M, Burris HA III, Rugo HS, Sahmoud T, et al. Everolimus in postmenopausal hormone-receptor-positive advanced breast cancer. N Engl J Med 2012;366:520–9.
13. Yao JC, Shah MH, Ito T, Bohas CL, Wolin EM, Van Cutsem E, et al. Everolimus for advanced pancreatic neuroendocrine tumors. N Engl J Med 2011;364:514–23.
14. Motzer RJ, Escudier B, Oudard S, Hutson TE, Porta C, Bracarda S, et al. Efficacy of everolimus in advanced renal cell carcinoma: a double-blind, randomised, placebo-controlled phase III trial. Lancet 2008;372:449–56.
15. Owonikoko TK, Khuri FR. Targeting the PI3K/AKT/mTOR Pathway. Am Soc Clin Oncol Educ Book 2013;2013:395–401.
16. Boulay A, Zumstein-Mecker S, Stephan C, Beuvink I, Zilbermann F, Haller R, et al. Antitumor efficacy of intermittent treatment schedules with the rapamycin derivative RAD001 correlates with prolonged inactivation of ribosomal protein S6 kinase 1 in peripheral blood mononuclear cells. Cancer Res 2004;64:252–61.
17. Nogova L, Boellaard R, Kobe C, Hoetjes N, Zander T, Gross SH, et al. Downregulation of 18F-FDG uptake in PET as an early pharmacodynamic effect in treatment of non-small cell lung cancer with the mTOR inhibitor everolimus. J Nucl Med 2009;50:1815–9.
18. Honer M, Ebenhan T, Allegrini PR, Ametamey SM, Becquet M, Cannet C, et al. Anti-angiogenic/vascular effects of the mTOR inhibitor everolimus are not detectable by FDG/FLT-PET. Transl Oncol 2010;3:264–75.

Published OnlineFirst February 11, 2015; DOI: 10.1158/1078-0432.CCR-14-1998

19. O'Donnell A, Faivre S, Burris HA III, Rea D, Papadimitrakopoulou V, Shand N, et al. Phase I pharmacokinetic and pharmacodynamic study of the oral mammalian target of rapamycin inhibitor everolimus in patients with advanced solid tumors. J Clin Oncol 2008;26:1588–95.
20. Tabernero J, Rojo F, Calvo E, Burris H, Judson I, Hazell K, et al. Dose- and schedule-dependent inhibition of the mammalian target of rapamycin pathway with everolimus: a phase I tumor pharmacodynamic study in patients with advanced solid tumors. J Clin Oncol 2008; 26:1603–10.
21. Kovarik JM, Eisen H, Dorent R, Mancini D, Vigano M, Rouilly M, et al. Everolimus in de novo cardiac transplantation: pharmacokinetics, therapeutic range, and influence on cyclosporine exposure. J Heart Lung Transplant 2003;22:1117–25.
22. Wahl RL, Jacene H, Kasamon Y, Lodge MA. From RECIST to PERCIST: Evolving Considerations for PET response criteria in solid tumors. J Nucl Med 2009;50 Suppl 1:122S–50S.
23. Brignol N, McMahon LM, Luo S, Tse FL. High-throughput semi-automated 96-well liquid/liquid extraction and liquid chromatography/mass spectrometric analysis of everolimus (RAD 001) and cyclosporin a (CsA) in whole blood. Rapid Commun Mass Spectrom 2001;15:898–907.
24. Detre S, Saclani Jotti G, Dowsett M. A "quickscore" method for immunohistochemical semiquantitation: validation for oestrogen receptor in breast carcinomas. J Clin Pathol 1995;48:876–8.
25. Su Z, Dias-Santagata D, Duke M, Hutchinson K, Lin YL, Borger DR, et al. A platform for rapid detection of multiple oncogenic mutations with relevance to targeted therapy in non-small-cell lung cancer. J Mol Diagn 2011;13:74–84.
26. Sun SY, Rosenberg LM, Wang X, Zhou Z, Yue P, Fu H, et al. Activation of Akt and eIF4E survival pathways by rapamycin-mediated mammalian target of rapamycin inhibition. Cancer Res 2005;65:7052–8.
27. O'Reilly KE, Rojo F, She QB, Solit D, Mills GB, Smith D, et al. mTOR inhibition induces upstream receptor tyrosine kinase signaling and activates Akt. Cancer Res 2006;66:1500–8.
28. Sequist LV, Waltman BA, Dias-Santagata D, Digumarthy S, Turke AB, Fidias P, et al. Genotypic and histological evolution of lung cancers acquiring resistance to EGFR inhibitors. Sci Transl Med 2011;3:75ra26.
29. Altorki N, Lane ME, Bauer T, Lee PC, Guarino MJ, Pass H, et al. Phase II proof-of-concept study of pazopanib monotherapy in treatment-naive patients with stage I/II resectable non-small-cell lung cancer. J Clin Oncol 2010;28:3131–7.
30. Tarhini A, Kotsakis A, Gooding W, Shuai Y, Petro D, Friedland D, et al. Phase II study of everolimus (RAD001) in previously treated small cell lung cancer. Clin Cancer Res 2010;16:5900–7.
31. Bergethon K, Shaw AT, Ou SH, Katayama R, Lovly CM, McDonald NT, et al. ROS1 rearrangements define a unique molecular class of lung cancers. J Clin Oncol 2012;30:863–70.
32. Lynch TJ, Bell DW, Sordella R, Gurubhagavatula S, Okimoto RA, Brannigan BW, et al. Activating mutations in the epidermal growth factor receptor underlying responsiveness of non-small-cell lung cancer to gefitinib. N Engl J Med 2004;350:2129–39.
33. Soda M, Choi YL, Enomoto M, Takada S, Yamashita Y, Ishikawa S, et al. Identification of the transforming EML4-ALK fusion gene in non-small-cell lung cancer. Nature 2007;448:561–6.
34. Iyer G, Hanrahan AJ, Milowsky MI, Al-Ahmadie H, Scott SN, Janakiraman M, et al. Genome sequencing identifies a basis for everolimus sensitivity. Science 2012;338:221.
35. Faber AC, Corcoran RB, Ebi H, Sequist LV, Waltman BA, Chung E, et al. BIM expression in treatment-naive cancers predicts responsiveness to kinase inhibitors. Cancer Discov 2011;1:352–65.
36. Kuroda J, Puthalakath H, Cragg MS, Kelly PN, Bouillet P, Huang DC, et al. Bim and Bad mediate imatinib-induced killing of Bcr/Abl+ leukemic cells, and resistance due to their loss is overcome by a BH3 mimetic. Proc Natl Acad Sci U S A 2006;103:14907–12.
37. Kuribara R, Honda H, Matsui H, Shinjyo T, Inukai T, Sugita K, et al. Roles of Bim in apoptosis of normal and Bcr-Abl-expressing hematopoietic progenitors. Mol Cell Biol 2004;24:6172–83.
38. Cragg MS, Kuroda J, Puthalakath H, Huang DC, Strasser A. Gefitinib-induced killing of NSCLC cell lines expressing mutant EGFR requires BIM and can be enhanced by BH3 mimetics. PLoS Med 2007;4:1681–89.
39. Costa DB, Halmos B, Kumar A, Schumer ST, Huberman MS, Boggon TJ, et al. BIM mediates EGFR tyrosine kinase inhibitor-induced apoptosis in lung cancers with oncogenic EGFR mutations. PLoS Med 2007;4:1669–79.
40. Ng KP, Hillmer AM, Chuah CT, Juan WC, Ko TK, Teo AS, et al. A common BIM deletion polymorphism mediates intrinsic resistance and inferior responses to tyrosine kinase inhibitors in cancer. Nat Med 2012; 18:521–8.
41. Engelman JA, Chen L, Tan X, Crosby K, Guimaraes AR, Upadhyay R, et al. Effective use of PI3K and MEK inhibitors to treat mutant Kras G12D and PIK3CA H1047R murine lung cancers. Nat Med 2008;14:1351–6.
42. Mahoney CL, Choudhury B, Davies H, Edkins S, Greenman C, Haaften G, et al. LKB1/KRAS mutant lung cancers constitute a genetic subset of NSCLC with increased sensitivity to MAPK and mTOR signalling inhibition. Br J Cancer 2009;100:370–5.
43. Ji H, Ramsey MR, Hayes DN, Fan C, McNamara K, Kozlowski P, et al. LKB1 modulates lung cancer differentiation and metastasis. Nature 2007; 448:807–10.

AACR American Association for Cancer Research

Clinical Cancer Research

A Translational, Pharmacodynamic, and Pharmacokinetic Phase IB Clinical Study of Everolimus in Resectable Non–Small Cell Lung Cancer

Taofeek K. Owonikoko, Suresh S. Ramalingam, Daniel L. Miller, et al.

Clin Cancer Res Published OnlineFirst February 11, 2015.